LAWRENCE
LIVERMORE
NATIONAL
LABORATORY

UCRL-JRNL-217732

Ion-Optics Calculations and Preliminary Precision Estimates of the Gas-Capable Ion Source for the 1-MV LLNL BioAMS Spectrometer

T. J. Ognibene, G. Bench, T. A. Brown, J. S. Vogel

December 14, 2005

Nuclear Instruments and Methods in Physics Research Sect. B

Ion-Optics Calculations and Preliminary Precision Estimates of the Gas-Capable Ion Source for the 1-MV LLNL BioAMS Spectrometer

T. J. Ognibene*, G. Bench, T. A. Brown and J. S. Vogel

Center for Accelerator Mass Spectrometry, Lawrence Livermore National Laboratory, 7000 East Ave, Livermore, CA 94551

*Corresponding author. Tel: 1-925-424-6266, email: ognibene1@llnl.gov

Abstract

Ion-optics calculations were performed for a new ion source and injection beam line. This source, which can accept both solid and gaseous targets, will be installed onto the 1-MV BioAMS spectrometer at the Center for Accelerator Mass Spectrometry, located at Lawrence Livermore National Laboratory and will augment the current LLNL cesium-sputter solid sample ion source. The ion source and its associated injection beam line were designed to allow direct quantification of $^{14}C/^{12}C$ and $^{3}H/^{1}H$ isotope ratios from both solid and gaseous targets without the need for isotope switching. Once installed, this source will enable the direct linking of a nanoflow LC system to the spectrometer to provide for high-throughput LC-AMS quantitation from a continuous flow. Calculations show that, for small samples, the sensitivity of the gas-accepting ion source could be precision limited but zeptomole quantitation should be feasible.

PACS: 07.05.Tp, 41.85.-p

Keywords: accelerator mass spectrometry, charged-particle optics, computer modeling, LC-AMS

Introduction

The 1-MV spectrometer at the Center for Accelerator Mass Spectrometry, located at Lawrence Livermore National Laboratory, is dedicated to the quantification of ^{14}C [1] and, recently, ^{3}H [2] within biochemical samples. Over 30,000 samples have been analyzed since operations began in May, 2001. High measurement throughput is enabled by the use of the LLNL high-output Cs-sputter solid sample ion source [3]. The use of solid targets necessitates the off-line conversion of biochemical samples to graphite [4] or TiH_2 [5]. Ion sources that are compatible with the direct input of biochemical separatory instrumentation, such as liquid chromatography, gas chromatography, capillary electrophoresis or other instruments would allow for real-time, automated sample preparation, potentially leading to increased resolution, improved sensitivity through reduced sample handling and the ability to do molecule-specific tracing of very small samples, but with a cost in precision. One such approach would involve the direct introduction of carbon, as CO_2, or hydrogen, as H_2, into the ion source. As the LLNL-designed ion source will only accept solid samples, a gas-accepting ion source was purchased from National Electrostatics Corporation (Middleton, WI). It is a modification of their cesium sputter ion source for solid targets and has been configured to accept both solid and gaseous samples [6]. This source, along with its associated injection beam line, will be mounted to the 1-MV AMS system through an existing port on a 45° electrostatic analyzer (ESA). The new injection beam line has been designed to allow for the direct quantification of either $^{14}C/^{12}C$ or $^{3}H/^{1}H$ isotopic ratios. Ion-optics calculations were performed to design the beam line to match

the phase space of the extracted ion beam to the acceptance of the accelerator. Additionally, preliminary precision estimates were calculated for quantification of ^{14}C from a continuous flow.

Description of the Beam Line

Figure 1 depicts a schematic representation of our planned installation together with the current bioAMS hardware [1]. Negative carbon ions extracted from the gas-capable ion source are focused through a 45° bending magnet with $^{12}C^-$ ions deposited onto a position-adjustable, off-axis Faraday cup. Extracted hydrogen ions are similarly transported to an off-axis Faraday cup for quantification of the $^{1}H^-$ ions located in a fixed position closer to the magnet. The transmitted rare ion beam will enter the 45° ESA for transport through the rest of the system to the rare isotope detector located at the end of the spectrometer. Presently, this detector consists of a single anode solid-state surface barrier detector. The field plates on the 45° ESA can be rotated by an externally controlled motor such that ions from either ion source may be transmitted to the rest of the spectrometer.

Ion Beam Envelope Calculations

PBO Lab 2.1.1 (AccelSoft, Inc., Delmar, CA), running on a x86 Family 6 Intel processor under Windows XP, was used to calculate ion beam envelopes from the ion source to the midpoint of the stripper canal. PBO Lab is a graphical user interface shell for use with several different particle optics design and analysis tools [7], including, TRACE 3-D. TRACE 3-D is a first-order beam dynamics program to calculate beam envelopes, using R-matrix formalism, through a user-defined ion transport system [8]. TRACE 3-D includes a linear approximation of space charge forces. As a result, for ion beams with a uniform charge distribution of ellipsoid

symmetry, the root mean squared (rms) properties can be replaced by an equivalent uniform beam. The net effect of this is that the total emittance of the equivalent uniform beam in each plane is five times its rms emittance, so that the beam envelopes in each plane are $\sqrt{5}$-times larger than their respective rms values.

Initial ion source terms and input parameters for the ion optical elements were provided by National Electrostatics Corporation or calculated. Results from beam envelope calculations of a $^{14}C^-$ beam are presented in Figure 2. Similar results are obtained with a $^{3}H^-$ ion beam. The transverse beam phase space plots in both the horizontal (solid line) and vertical (dashed line) are shown at the source (upper left plot) and at the midpoint of the stripper canal (upper right plot). Data relating to the longitudinal phase planes are not plotted as the beam bunch has been stretched in the z-direction to model a DC beam [9]. The two independent Twiss parameters, A and B, are also shown. The diameter of the beam spot size at the midpoint of the stripper canal is calculated to be 3.5 mm in the horizontal direction and 3.9 mm in the vertical direction; much smaller than the 5 mm diameter stripper canal.

The calculated equivalent uniform beam envelope half-widths through the ion transport system are shown in two plots on the bottom of Figure 2, with the horizontal plane displayed in the top half and the vertical plane on the bottom half. The full scale of each plot is 25 mm. The identities of the major beam line components are annotated. Note that the boxes designating the beam line components are not drawn to scale and that at no point does the ion beam size exceed the inner dimensions of the ion optical elements. The entrance and exit apertures of each acceleration gap was set to 0 mm to negate any TRACE 3-D-calculated fringe field effects. Instead, a thin lens was inserted to handle the focusing properties resulting from the change in the voltage gradient seen by the ion beam [10].

As can be seen from the traces, the two einzel lens work as a zoom lens with the entrance lens of the acceleration gap to focus the ion beam through the 45° bending magnet to a waist approximately mid way between the magnet and the 45° ESA. The two einzel lens telescope allows flexibility in the precise placement of this waist to accommodate changes in the ion source's emittance. This waist is positioned such that the ion beam has the correct divergence at the entrance to the first acceleration column to bring the beam to a parallel focus at the midpoint of the gas stripper canal. This waist after the 45° magnet must also be far enough away to allow for adequate separation of the $^{12}C^-$ ion beam to enable accurate quantitation. However, the further from the magnet that the waist is formed, the larger the spot size at that object point. A tradeoff has been made between these two conflicting properties and the available space within the laboratory. Based on the model, at the object plane of the magnet, the ion beams of the three isotopes of carbon are physically separated from each other by approximately 15 times greater than their respective beam radii.

Magnetic Field Calculations

The 45° bend magnet purchased from NEC is a reversed switching magnet with a radius of curvature of 275 mm for the central trajectory. While this configuration is adequate for the separation of carbon isotopes, there were concerns regarding its suitability for hydrogen isotope separation since this ion source and injection beam line will also be used for the quantification of ^3H from either gaseous H_2 or solid TiH_2 targets. Simple geometrical calculations indicated that with the magnet tuned to bend $^3H^-$ ions 45°, the $^1H^-$ ions would exit near the corner of the pole. The paths of ions exiting from a corner or a side of the pole would be exposed to severe defocusing magnetic fields that could interfere with accurate and precise quantification of $^1H^-$.

To more accurately model this potential problem, a grid-point mesh of the magnetic poles of the magnet was constructed using the ion-optics simulation code, SIMION 3D [11], running under the same computer platform as the beam envelope calculations. The magnetic field was established such that 60 keV $^{3}H^{-}$ ions, in the midplane of the magnet (entering with an edge angle of 22.5°), would be deflected 45° and exit the magnet perpendicular to the field. The physical size of the model was established such that the magnetic field could extend out to ~0.04% of its maximum value. Figure 3 shows the region around the magnet with views of the calculated paths of the central trajectories of $^{3}H^{-}$ and $^{1}H^{-}$ ions. Figure 3a shows the profile of the magnet pole pieces while Figure 3b is a top view of the ion paths.

The deflection angle of the $^{1}H^{-}$ ions is determined to be 72°, consistent with geometrical calculations. While the central trajectory of the $^{1}H^{-}$ ions does exit the magnet at the rear face, the entire beam envelope does not. However, the shape of the magnet pole extends the magnetic field such that most of the beam envelope will exit the field with an edge angle of ~27°. With this configuration, the ions are brought to a double focus 204 mm downstream of the magnet, at the location of the ^{1}H Faraday cup. For ions that exit more towards the side of the magnet, the edge angle begins to decrease. This perturbs the double focus such that the divergence of the ions in the horizontal dimension increases while the ions in the vertical dimension decreases. However, this does not present a serious problem, as this beam is only transported to the ^{1}H cup, which has been designed specifically to accept the resulting beam envelope.

Continuous Flow-Liquid Chromatography-AMS

One use of this new ion source is to couple a nano-flow liquid chromatography (LC) system to the spectrometer through an online combustion/oxidation interface. This interface will

directly inject CO_2 or H_2O from small, well-defined biochemical samples, for quantification of either ^{14}C or ^{3}H. The flow rates of the mobile phase in a nano-flow LC system may be low enough to enable its direct injection into the ion source after it has been converted to either CO_2 or H_2O. Increasing the CO_2 flow rate improves ion source output and efficiency up to a certain point, however, this performance begins to decrease with a further increase in the gas flow [12]. This system will also require the use of a carrier gas, such as helium or argon. Low carrier gas flow rates (on the order of a few hundred microliters per minute) have been shown to have no significant deleterious effect on ion source performance [13-15]. Quantification of a transient pulse within a continuous flow (CF) will potentially improve sensitivity, maximize separatory time resolution, increase measurement throughput and reduce costs. However, precision will ultimately be a function of the peak width from the LC and not a function of measurement time (as is the case for solid targets). Any gas, that is not ionized, will be immediately pumped out by the vacuum system and lost to further measurement.

To illustrate this concept, the expected precision in quantification of ^{14}C with respect to sample size was estimated from sample counting statistics [16]. The count rate in a single anode detector will be a combination of true ^{14}C events (^{14}C) from the sample pulse and scattered events ("^{14}C") that are indistinguishable from true ^{14}C events. The main source of these scattered events will likely arise from the combusted mobile phase. This scattering will consist of scatter from injected carbon and scattering from the low-energy tails of potentially intense $^{16}O^-$ beams.

As the gas-accepting ion source is not yet operational, the expected amount of scattered ions reaching the detector from injected CO_2 was estimated assuming a linear combination of scatter from carbon and oxygen in solid targets. An upper bound of the scattering from carbon was determined to ~2.4×10^{-15} "^{14}C"/C from measurements of solid graphite samples prepared

from coal [2]. The scattering contribution from oxygen was determined based on measurements of solid samples consisting of well-defined mixtures of -200 mesh graphite and TiO_2 powders. Samples containing C:O (mole:mole) ratios ranging from 0 (in the case of pure TiO_2) to 2 were prepared and the total ^{14}C count rate in the detector, as well as the $^{13}C^+$, $^{12}C^-$ and $^{16}O^-$ ion currents were measured on the 1-MV AMS spectrometer. After subtracting the contribution of ^{14}C (both real and scatter) from the graphite portion of the samples and normalizing to the analyzed $^{16}O^-$ ion current, the scattering from oxygen was estimated to be $(4\pm1)x10^{-15}$ "^{14}C"/O. During these tests, the oxygen sputtering yield was ~1 order of magnitude greater than the carbon sputtering yield. Although higher sputtering yields from oxygen are expected due to its larger electron affinity over that of carbon, this yield is higher than a previously reported observation by a factor of ~5 [17]. This difference may arise, in part, to differences between solid and gas samples suggesting that scattering results from the graphite:TiO_2 sample matrix may represent an upper bound to that expected from CO_2 gas. With this caveat, the total amount of scatter ions from injected CO_2 reaching the detector is estimated to be $\sim1x10^{-14}$ "^{14}C"/CO_2.

The carbonaceous component of a mobile phase for a typical nano-flow LC system is acetonitrile with a flow of 50 nl min^{-1}. Under Standard Laboratory Conditions (25°C, 100 kPa), this yields ~0.08 µl CO_2 sec^{-1} entering the ion source, assuming the combustion/oxidation interface operates with 100% efficiency and a 1:10 open split in the gas flow. This flow rate is comparable to those used in other AMS gas-accepting ion sources [15,18]. The use of an open split, however, reduces the overall precision and will be avoided, if possible. Using the split gas flow rate, a 10% ion source efficiency [19] and a 36% typical transmission through the spectrometer [2], the amount of scattered ions striking the ^{14}C detector can be calculated.

Similarly, the number of ^{14}C ions, from an assumed peak in the LC trace, striking the detector can also be calculated.

The result of this calculation is presented in Figure 4. The precision is presented as the calculated error in the amount of ^{14}C relative to the total amount of ^{14}C contained in a 30 second wide LC peak. For comparison, the precision in the absence of any scattering background is also shown. For both of these curves, background sources of true ^{14}C in the solvent or sample are considered insignificant. Setting a precision threshold of 10%, samples must contain at least 200 zeptomole ^{14}C to derive meaningful conclusions. In the absence of scattering, the minimum amount is reduced to ~50 zmol and represents a best case for this scenario. As the amount of ^{14}C in the sample increases, background scatter becomes less significant. As an example, the detector count rate from a sample containing 2.5 amol ^{14}C is more than 1000 times greater than the scatter count rate.

One way to improve the precision for a sample would be to shorten the width of the LC peak. This can be achieved by increasing the LC flow rate. However, with the current flow rate, it is likely that a flow splitter will be employed and any increase in the LC flow rate will increase the amount of CO_2 generated which will require a larger split before entering the ion source. An increase in the size of the split will reduce the amount of the analyte entering the source, which will reduce the measured precision. Increasing the efficiency of the ion source will also allow a reduction in the minimum sample size that can be measured with an acceptable precision. Of course, experimental precision can be improved by the measurement of replicate samples. Additionally, replacing the single anode solid-state surface barrier detector with a gas proportional counter with a very thin Si_3N_4 entrance window could allow for particle identification and rejection of a significant portion of non-^{14}C ions reaching the detector [20].

Detector count rates may ultimately determine the maximum amount of ^{14}C in a sample that may be quantified as corrections for electronic livetime become less reliable at higher count rates. In a single anode detector, the total count rate from a sample containing 700 amol ^{14}C, could exceed 50 kHz. This suggests the need for a fast particle counter such as those based on electron multipliers [21]. Quantitation of a widely varying range of count rates may have to be resolved by the construction of a hybrid detector system.

Conclusions

Prior to installation onto our existing AMS system, the ion source and injection beam line are being assembled in the main accelerator hall. Additional beam profile monitors, slits and Faraday cups have been installed after the 45° magnet. Using both solid and gaseous targets, ion source performance and ion beam transport will be assessed. If necessary, both will be modified to maximize output and ion transmission. These results will also be compared to the ion optics calculations to guarantee optimal coupling to the existing spectrometer. Development of an online combustion system will proceed in parallel to the installation

One immediate application of this instrumentation is to quantify metabolite profiles in single cells. These experiments require relatively high degrees of specific isotope labeling. However, the size of an individual cell limits the total amount of ^{14}C that may be incorporated and, hence, quantified. Also, high analysis throughput will be required to establish meaningful statistics from many individual single cells.

Acknowledgements

Work performed (partially) at the Research Resource for Biomedical AMS which is operated by UC, LLNL under the auspices of the U.S. Department of Energy under contract #W-7405-ENG-48. The Research Resource is supported by the National Institutes of Health, National Center for Research Resources, Biomedical Technology Program grant #P41 RR13461.

References

[1] T.J. Ognibene, G. Bench, T.A. Brown, G.F. Peaslee, and J.S. Vogel, Int. J. Mass Spectrom. 218 (2002) 255.

[2] T.J. Ognibene, G. Bench, T.A. Brown, and J.S. Vogel, Nucl. Instr. and Meth. B 223-224 (2004) 12.

[3] J. Southon and M. Roberts, Nucl. Instr. and Meth. B 172 (2000) 257.

[4] T.J. Ognibene, G. Bench, J.S. Vogel, G.F. Peaslee, and S. Murov, Anal. Chem. 75 (2003) 2192.

[5] M.L. Chiarappa-Zucca, K.H. Dingley, M.L. Roberts, C.A. Velsko, and A.H. Love, Anal. Chem. 74 (2002) 6285.

[6] J.A. Ferry, R.L. Loger, G.A. Norton, and J.E. Raatz, Nucl. Instr. and Meth. A 382 (1996) 316.

[7] G.H. Gillespie, B.W. Hill, H. Martono, and J.M. Moore, Nucl. Instr. and Meth. B 161 (2000) 1168.

[8] K.R. Crandall and D.P. Rusthoi, TRACE 3-D Documentation, LA-UR-97-986, Los Alamos National Laboratory (1997).

[9] G.H. Gillespie, in: C.E. Eyberger, R.C. Pardo and M.M. White (eds.) Proceedings of the *XIXth International Linear Accelerator Conference*, Chicago, Illinois, USA, (Argonne National Laboratory, 1998) ANL-98/28, 150.

[10] T.J. Ognibene, T.A. Brown, J.P. Knezovich, M.L. Roberts, J.R. Southon, and J.S. Vogel, Nucl. Instr. and Meth. B 172 (2000) 47.

[11] D.A. Dahl, Simion 3D Version 7.0, INEEL-95/0403, Idaho National Engineering and Environmental Laboratory (2000).

[12] C.R. Bronk and R.E.M. Hedges, Nucl. Instr. and Meth. B 29 (1987) 45.

[13] C. Bronk Ramsey, P. Ditchfield, and M. Humm, Radiocarbon 47 (2004) 25.

[14] B.J. Hughey, P.L. Skipper, R.E. Klinkowstein, R.E. Shefer, J.S. Wishnok, and S.R. Tannenbaum, Nucl. Instr. and Meth. B 172 (2000) 40.

[15] T. Uhl, W. Kretschmer, W. Luppold, and A. Scharf, Radiocarbon 46 (2004) 65.

[16] J.S. Vogel, T. Ognibene, M. Palmblad, and P. Reimer, Radiocarbon 46 (2004) 1103.

[17] C.R. Bronk and R.E.M. Hedges, Radiocarbon 31 (1989) 298.

[18] C.B. Ramsey and R.E.M. Hedges, Radiocarbon 37 (1995) 711.

[19] J.A. Ferry, National Electrostatics Corporation, personal communication.

[20] H.-A. Synal, these proceedings

[21] S. Richter, S.A. Goldberg, P.B. Mason, A.J. Traina, and J.B. Schwieters, Int. J. Mass Spectrom. 206 (2001) 105.

Figure Captions

Figure 1. Schematic layout of the LLNL 1-MV AMS system for quantification of ^{14}C and ^{3}H in biochemical samples. The new gas-capable ion source and its associated beam line (highlighted with a dashed ellipse) will attach to an existing port on the 45° ESA to augment the current LLNL AMS ion source.

Figure 2. Ion beam envelope calculations of ^{14}C ions extracted from the new ion source and transported to the midpoint of the gas stripper canal at the center of the tandem accelerator. Similar results were obtained for ^{3}H ion beams. See text for details.

Figure 3. Calculated ion trajectories through the 45° magnet on the new beam line showing an isometric view (3a) and vertical view (3b) of the paths of the $^{3}H^{-}$ and $^{1}H^{-}$ central rays.

Figure 4. Calculated precision based on counting statistics with respect to the amount of ^{14}C in a 30 second wide peak eluting from a liquid chromatography system in a continuous flow AMS application. The two curves present two cases: that of no scatter component (dashed line) and that of scatter from injected CO_2 (solid line) in the measured detector signal. See text for details.

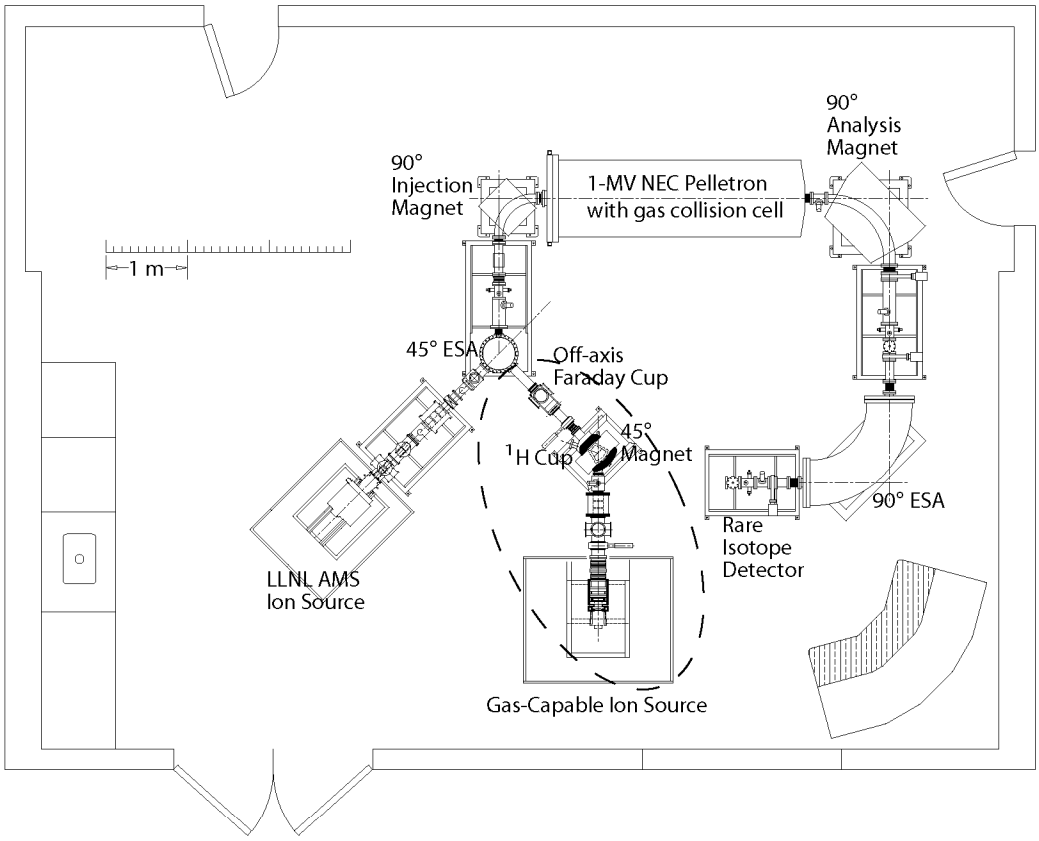
90°
Analysis
Magnet
90°
Injection
Magnet
1-MV NEC Pelletron
with gas collision cell
1 m
45° ESA
Off-axis
Faraday Cup
45°
Magnet
^{1}H Cup
90° ESA
Rare
Isotope
Detector
LLNL AMS
Ion Source
Gas-Capable Ion Source

Figure 1

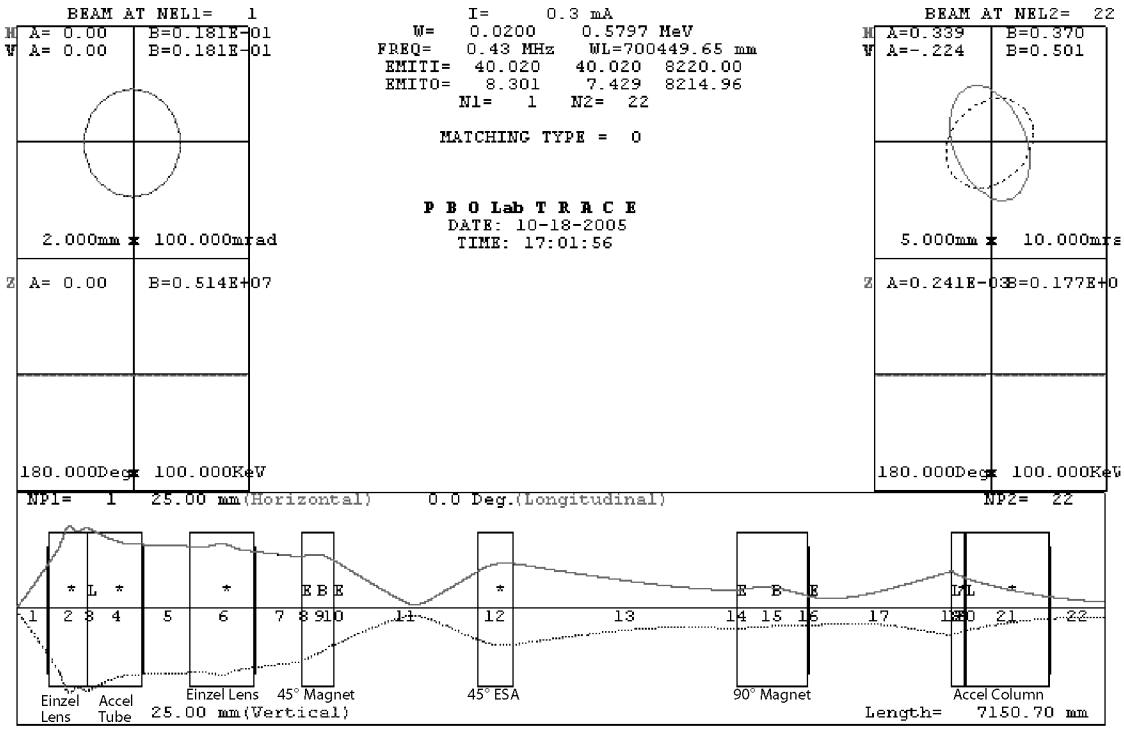
BEAM AT NEL1= 1
H A= 0.00 B=0.181E-01
V A= 0.00 B=0.181E-01
2.000mm x 100.000mrad
Z A= 0.00 B=0.514E+07
180.000Deg x 100.000KeV
I= 0.3 mA
W= 0.0200 0.5797 MeV
FREQ= 0.43 MHz WL=700449.65 mm
EMITI= 40.020 40.020 8220.00
EMITO= 8.301 7.429 8214.96
N1= 1 N2= 22
MATCHING TYPE = 0
P B O Lab T R A C E
DATE: 10-18-2005
TIME: 17:01:56
BEAM AT NEL2= 22
H A=0.339 B=0.370
V A=-.224 B=0.501
5.000mm x 10.000mra
Z A=0.241E-03 B=0.177E+0
180.000Deg x 100.000KeV
NP1= 1 25.00 mm(Horizontal) 0.0 Deg.(Longitudinal) NP2= 22
Einzel Lens
Accel Tube
Einzel Lens
45° Magnet
45° ESA
90° Magnet
Accel Column
25.00 mm(Vertical)
Length= 7150.70 mm

Figure 2

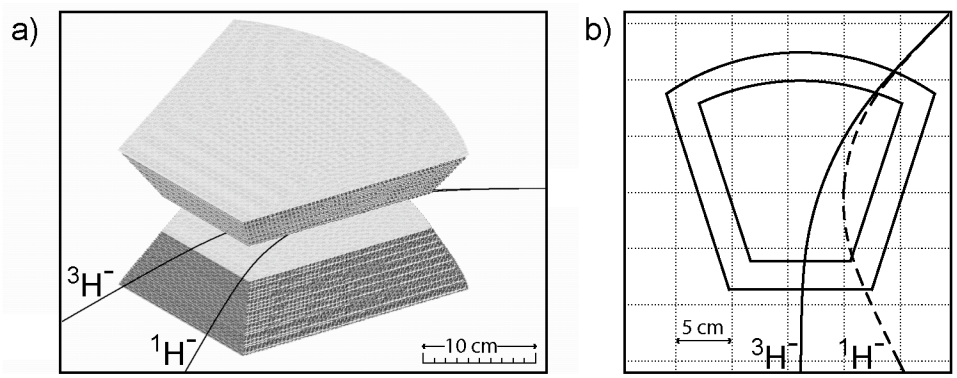

Figure 3.

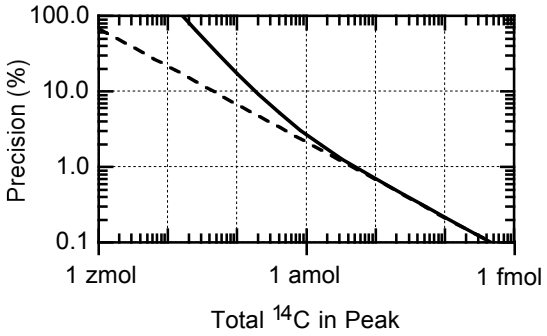

Figure 4